Proceedings of the 2007 American Control Conference
Marriott Marquis Hotel at Times Square
New York City, USA, July 11-13, 2007

Stabilization of Cascaded Systems via $\mathcal{L}_1$ Adaptive Controller with Application to a UAV Path Following Problem and Flight Test Results

Chengyu Cao, Naira Hovakimyan, Isaac Kaminer, Vijay V. Patel and Vladimir Dobrokhodov

Abstract— **This paper presents a theoretical framework for augmenting an existing autopilot by an adaptive element so that it tracks a given smooth reference command with desired specifications. The main contribution of the approach is that it allows for augmenting the autopilot without any modifications to it. The augmentative adaptive element is based on the $\mathcal{L}_1$ adaptive output feedback control architecture developed in [1]. The complete path following architecture of this paper enables a UAV with an off-the-shelf autopilot to follow a predetermined path that it was not otherwise designed to follow. The paper concludes with flight test results performed in Camp Roberts, CA, in February of 2007.**

I. Introduction

This paper develops a theoretical framework for augmenting the existing autopilot for a single unmanned aerial vehicle (UAV), which is tasked to follow a certain trajectory with prespecified tight bounds. The problem in this paper was motivated by the framework of [2] for coordinated path following of multiple vehicles under spatial and temporal constraints. Examples of various missions include coordinated ground target suppression and sequential auto-landing for multiple UAVs per se. Both mission scenarios require a group of UAVs to execute time-critical maneuvers in close proximity of each other. While Ref. [2] presents a guidance framework for time-critical coordination of multiple UAVs, this paper presents an adaptive control architecture to ensure that an existing autopilot for a single UAV can execute the specified path with sufficient accuracy. For that purpose, we use the framework of the recent $\mathcal{L}_1$ adaptive control architecture [3], [4] and its extension to output feedback [1], [5] that enables augmentation of the autopilot without any modifications to it. The complete path following architecture of this paper enables a UAV with an off-the-shelf autopilot to follow a predetermined path that it was not otherwise designed to follow. Additionally, the $\mathcal{L}_1$ adaptive augmentation leads to analytically computable performance bounds for both input and output signals simultaneously [6], [7]. In [8], we report the extension of this framework to a fleet of UAVs that enables cooperative control for time-critical missions, and we correspondingly extend the stability proof from [2] to account for the adaptive augmentation.

The paper is organized as follows. Section II states the problem formulation. Section III describes the kinematics of the path following algorithm. Section IV summarizes the overall control architecture, while Section V verifies the theoretical findings with results from real flight tests performed in Camp Roberts, CA, in February of 2007. Section VI concludes the paper. Throughout the paper $\|\cdot(s)\|_{\mathcal{L}_1}$ will denote the $\mathcal{L}_1$ gain of the system, while $\|\cdot\|_{\mathcal{L}_\infty}$ will denote the $\mathcal{L}_\infty$ norm of the signal.

Research is supported by ONR under Contract N00014-05-1-0828 and AFOSR under Contract No. FA9550-05-1-0157.

C. Cao, V. Patel, N. Hovakimyan are with Aerospace & Ocean Engineering, Virginia Polytechnic Institute & State University, Blacksburg, VA 24061-0203, e-mail: {chengyu, nhovakim, vvp2069}@vt.edu, while I. Kaminer and V. Dobrokhodov are with Naval Postgraduate School, Monterey, CA 93943, e-mail: {kaminer, vldobr}@nps.edu

II. Problem Formulation

In this paper we consider the problem of stabilization of cascaded systems given by:

$$\mathcal{G}_e: \quad \dot{x}(t) = f(x(t)) + g(x(t))y(t) \tag{1}$$

$$\mathcal{G}_p: \quad y(s) = G_p(s)(u(s) + z(s)), \tag{2}$$

where the subsystem $\mathcal{G}_e$ represents the path-following kinematics of the UAV, while the subsystem $\mathcal{G}_p$ models the closed-loop system of the UAV with the autopilot. Figure 1 presents a sketch of this cascaded system. We note that $x(t)$ and $y(t)$ are the measured outputs of this cascaded system, $u(t)$ is the only control signal, and $y(s)$, $u(s)$ denote the Laplace transforms of $y(t)$ and $u(t)$ respectively. The maps f, g are known, $G_p(s)$ is unknown strictly proper transfer function, and $z(s)$ is the Laplace transform of $z(t)$, which models the unknown bounded time-varying disturbances. The control objective is to stabilize $x(t)$ by the design of $u(t)$ without any modifications to the autopilot. Below we characterize both subsystems separately.

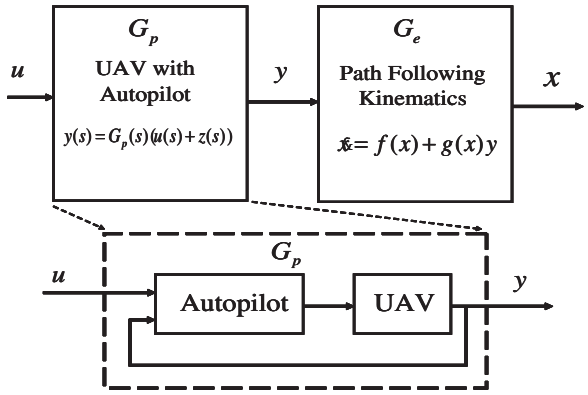

Fig. 1. Cascaded systems

III. Existence of a Stabilizing Function for the Kinematics of Path Following

Let F be a Serret-Frenet frame, Fig. 2, attached to a generic point on the path, and let W be the wind frame

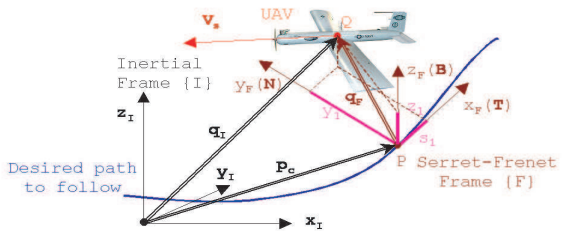

Fig. 2. Cascaded systems

attached to the UAV (a frame that has its x-axis aligned with the UAV's velocity vector). Let $p_c(\tau)$ be a desired trajectory to be followed by a single UAV, where τ denotes the path length. Let

$$q_I = [x_I \; y_I \; z_I]^\top \tag{3}$$

be the position of the aircraft center of mass resolved in I. Let $q_F = [x_F \; y_F \; z_F]^\top$ be the difference between q_I and p_c resolved in F. Furthermore, let ψ_e, θ_e, ψ_e denote the Euler angles that locally parameterize the rotation matrix from F to W. Let

$$x(t) = [x_F(t) \;\; y_F(t) \;\; z_F(t) \;\; \theta_e(t) - \delta_\theta(t) \;\; \psi_e(t) - \delta_\psi(t)]^\top,$$

where

$$\begin{aligned} \delta_\theta(t) &= \sin^{-1}\left(\frac{z_F(t)}{|z_F(t)| + d_1}\right), \\ \delta_\psi(t) &= \sin^{-1}\left(\frac{y_F(t)}{|y_F(t)| + d_2}\right), \end{aligned} \tag{4}$$

with $d_1 > 0$, $d_2 > 0$ being some constants, and $v(t)$ be the UAV speed subject to the following lower bound:

$$v(t) \geq v_{\min}, \quad \forall\, t \geq 0\,. \tag{5}$$

It follows from [2] that the open-loop system $\mathcal{G}_e$, describing the kinematic error equations of a UAV, is given by:

$$\mathcal{G}_e: \begin{array}{l} \dot{x}_F(t) = -\dot{\tau}(t)(1 - \kappa(\tau(t))y_F(t)) + v\cos(\theta_e(t))\cos(\psi_e(t)) \\ \dot{y}_F(t) = -\dot{\tau}(t)(\kappa(\tau(t))x_F(t) - \zeta(\tau(t))z_F(t)) + \\ \qquad v\cos(\theta_e(t))\sin(\psi_e(t)) \\ \dot{z}_F(t) = -\zeta(\tau(t))\dot{\tau}(t)y_F(t) - v\sin(\theta_e(t)) \\ \dot{\theta}_e(t) = u_\theta(t) \\ \dot{\psi}_e(t) = u_\psi(t) \\ \dot{\tau}(t) = K_1 x_F(t) + v\cos(\theta_e(t))\cos(\psi_e(t)) \\ y(t) = [u_\theta(t) \; u_\psi(t)]^\top, \end{array} \tag{6}$$

where $K_1 > 0$, $\kappa(\tau)$ and $\zeta(\tau)$ denote the curvature and torsion of the desired path $p_c(\tau)$ respectively, and $y(t)$ is the vector of the input signals of the system $\mathcal{G}_e$. First we prove that in the absence of $\mathcal{G}_p$ there exist stabilizing functions for the system $\mathcal{G}_e$ leading to local exponential stability with a prescribed domain of attraction. Towards that end, let c_1 and c_2 be related as follows:

$$\sqrt{2cc_2} + \sin^{-1}\left(\frac{2cc_1}{d_1 + \sqrt{2cc_1}}\right) < \frac{\pi}{2}\,, \tag{7}$$

where $c > 0$ is any positive constant, and let $y_c(t) = [u_{\theta_c}(t) \; u_{\psi_c}(t)]^\top$ with

$$\begin{aligned} u_{\theta_c}(t) &= -K_2(\theta_e(t) - \delta_\theta(t)) + \frac{c_2}{c_1} z_F(t) v(t) \\ &\quad \frac{\sin(\theta_e(t)) - \sin(\delta_\theta(t))}{\theta_e(t) - \delta_\theta(t)} + \dot{\delta}_\theta(t) \\ u_{\psi_c}(t) &= -K_3(\psi_e(t) - \delta_\psi(t)) - \frac{c_3}{c_1} y_F(t) v(t) \\ &\quad \cos(\theta_e(t)) \frac{\sin(\psi_e(t)) + \sin(\delta_\psi(t))}{\psi_e(t) - \delta_\psi(t)} + \dot{\delta}_\psi, \end{aligned} \tag{8}$$

where $K_2 > 0, K_3 > 0$. It follows from [2] that the system in (6) can be stabilized by the functions in (8). The next lemma follows from the main result in [2].

Lemma 1: Let $d_1 = d_2 = d$, where d_1, d_2 are in introduced in (4), and $c = 2c_1 d$. Then the closed-loop system in (6), (8) is locally exponentially stable with the domain of attraction

$$\Omega = \left\{ x : V_c(x) \leq \frac{d^2}{2c_1} \right\},$$

where

$$\begin{aligned} V_c(x(t)) &= x^\top(t) P x(t)\,, \\ P &= \operatorname{diag}\left(\frac{1}{2c_1} \; \frac{1}{2c_1} \; \frac{1}{2c_1} \; \frac{1}{2c_2} \; \frac{1}{2c_3}\right), \end{aligned} \tag{9}$$

and $c_3 > 0$ is any positive constant.

Proof. It follows from (6) and (8) that

$$\begin{aligned} &\dot{V}_c(x(t)) = \frac{x_F}{c_1}(-\dot{\tau}(1 - \kappa(\tau)y_F) + v\cos(\theta_e)\cos(\psi_e)) \\ &+\frac{y_F}{c_1}(-\dot{\tau}(\kappa(\tau)x_F - \zeta(\tau)z_F + v\cos(\theta_e)\sin(\psi_e))) \\ &+\frac{z_F}{c_1}(-\zeta(\tau)\dot{\tau}y_F - v\sin(\theta_e)) + \frac{\theta_e - \delta_\theta}{c_2}(u_{\theta_c}(t) - \dot{\delta}_\theta) \\ &+\frac{\psi_e - \delta_\psi}{c_3}(u_{\psi_c} - \dot{\delta}_\psi) \\ &= \frac{-x_F\dot{\tau} + v\cos(\theta_e)(x_F\cos(\psi_e) + y_F\sin(\psi_e))}{c_1} \\ &+\frac{-z_F v\sin(\theta_e)}{c_1} - \frac{K_2}{c_2}(\theta_e - \delta_\theta)^2 - \frac{K_3}{c_3}(\psi_e - \delta_\psi)^2 + \\ &\frac{v z_F(\sin(\theta_e) - \sin(\delta_\theta))}{c_1} \\ &-\frac{y_F v\cos(\theta_e)(\sin(\psi_e) + \sin(\delta_\psi))}{c_1} \\ &= -\frac{K_1}{c_1}x_F^2 - \frac{K_2}{c_2}(\theta_e - \delta_\theta)^2 - \frac{K_3}{c_3}(\psi_e - \delta_\psi)^2 \\ &-\frac{v y_F\sin(\delta_\psi)\cos(\theta_e) + v z_F\sin(\delta_\theta)}{c_1} \end{aligned} \tag{10}$$

Using (4), we have

$$\begin{aligned} &\dot{V}_c(t) = -\frac{K_1}{c_1}x_F^2 - \frac{K_2}{c_2}(\theta_e - \delta_\theta)^2 - \frac{K_3}{c_3}(\psi_e - \delta_\psi)^2 \\ &-\frac{v z_F^2}{c_1(|z_F| + d_1)} - \frac{v\cos(\theta_e)y_F^2}{c_1(|y_F| + d_2)} = -x^\top Q x\,, \end{aligned} \tag{11}$$

where

$$Q = \mathrm{diag}\left(\frac{K_1}{c_1} \;\; \frac{v\cos(\theta_e)}{c_1(|y_F|+d_2)} \;\; \frac{v}{c_1(|z_F|+d_1)} \;\; \frac{K_2}{c_2} \;\; \frac{K_3}{c_3}\right). \tag{12}$$

We note that $Q > Q_c$, where

$$\begin{aligned} Q_c \;\; = \;\; & \mathrm{diag}\Big(\frac{K_1}{c_1} \;\; \frac{v_{\min}}{c_1(|y_{F_{\max}}|+d_2)} \\ & \frac{v_{\min}}{c_1(|z_{F_{\max}}|+d_1)} \;\; \frac{K_2}{c_2} \;\; \frac{K_3}{c_3}\Big) \end{aligned} \tag{13}$$

Since $Q_c > 0$ and

$$\dot{V}_c(t) \leq -x^\top(t) Q_c x(t) \quad \forall\, t \geq 0\,, \tag{14}$$

then $x(t)$ is exponentially stable over the compact set Ω, which completes the proof.

□

IV. $\mathcal{L}_1$ ADAPTIVE CONTROL OF CASCADED SYSTEMS

A. UAV with Autopilot

The system $\mathcal{G}_p$ represents the closed-loop autopilot of the UAV with the input $u(t) = [u_1(t) \;\; u_2(t)]^\top$ and the output $y(t) = [u_\theta(t) \;\; u_\psi(t)]^\top$. The subsystem $\mathcal{G}_p$ can be described as

$$\mathcal{G}_p: \;\; \begin{array}{l} u_\theta(s) = G_{p1}(s)(u_1(s) + z_1(s)) \\ u_\psi(s) = G_{p2}(s)(u_2(s) + z_2(s))\,, \end{array} \tag{15}$$

where $G_{p1}(s)$ and $G_{p2}(s)$ are unknown strictly proper transfer functions, $z_1(s)$ and $z_2(s)$ represent the Laplace transformation of the signals $z_1(t)$ and $z_2(t)$, respectively. We note that the autopilot is designed to ensure that $y(t)$ tracks any smooth $u(t)$ in the absence of $\mathcal{G}_e$. We further assume that the time-varying disturbances are bounded functions of time with uniformly bounded derivatives:

$$|z_i(t)| \;\; \leq \;\; L_{i0}\,, \quad i = 1, 2\,, \tag{16}$$

$$|\dot{z}_i(t)| \;\; \leq \;\; L_{i1}\,, \quad i = 1, 2\,. \tag{17}$$

where L_{i0}, L_{i1} are some conservative known bounds.

Remark 1: We notice that the bandwidth of the control channel of the closed-loop UAV with the autopilot is very limited, and the model (15) is valid only for low-frequency approximation of $\mathcal{G}_p$.

We note that only very limited knowledge of the autopilot is assumed at this point. We do not assume knowledge of the state dimension of the unknown transfer functions $G_{pi}(s)$, $i = 1, 2$. We only assume that these are strictly proper transfer functions.

Next, we isolate the autopilot with the UAV to design an adaptive controller for it to track any desired bounded continuous reference input. Upon that, we consider stabilization of the cascaded system.

Notice that since $y_c(t)$ stabilizes the subsystem $\mathcal{G}_e$, the control objective for the subsystem $\mathcal{G}_p$ is reduced to designing an adaptive output feedback controller $u(t)$ such that output $y(t)$ tracks the reference input $y_c(t)$ following a desired reference model, i.e.

$$u_\theta(s) \;\; \approx \;\; M(s) u_{\theta_c}(s)\,, \tag{18}$$

$$u_\psi(s) \;\; \approx \;\; M(s) u_{\psi_c}(s)\,. \tag{19}$$

In this paper, for simplicity we consider a first order system, i.e. we set

$$M(s) = \frac{m}{s+m}\,, \quad m > 0. \tag{20}$$

Since the systems in (18) and (19) have the same structure, we define the $\mathcal{L}_1$ adaptive control architecture only for the system in (18). The same analysis and design can be applied to the system in (19).

B. $\mathcal{L}_1$ adaptive controller

The elements of $\mathcal{L}_1$ adaptive controller for the system in (15) are introduced below.

State Predictor: We consider the state predictor:

$$\dot{\hat{u}}_\theta(t) = -m\hat{u}_\theta(t) + m\left(u_1(t) + \hat{\sigma}(t)\right), \;\; \hat{u}_\theta(0) = 0\,, \tag{21}$$

where the adaptive estimate $\hat{\sigma}(t)$ is governed by the following adaptation law.

Adaptive Law: The adaptation of $\hat{\sigma}(t)$ is defined as:

$$\dot{\hat{\sigma}}(t) = \Gamma_c \mathrm{Proj}(\hat{\sigma}(t), -(\hat{u}_\theta(t) - u_\theta(t))), \;\; \hat{\sigma}(0) = 0, \tag{22}$$

where $\Gamma_c \in \mathbb{R}^+$ is the adaptation rate, while projection is performed on a compact set which is large enough to encompass the possible uncertainties. Quantitative analysis on the choice of Γ_c and other design details can be found in [1], [5].

Control Law: The control signal is generated by:

$$u_1(s) \;\; = \;\; u_{\theta_c}(s) - C(s)\hat{\sigma}(s)\,, \tag{23}$$

where $C(s)$ is a strictly proper system with $C(0) = 1$, and $u_{\theta_c}(t)$ is the output of the stabilization function in (8). In this paper, we consider the simplest choice of a first order low-pass filter:

$$C(s) = \frac{\omega}{s+\omega}\,. \tag{24}$$

The complete $\mathcal{L}_1$ adaptive controller consists of (21), (22) and (23) subject to the following $\mathcal{L}_1$-gain stability requirement [1], [5].

$\mathcal{L}_1$-gain stability requirement: $C(s)$ and $M(s)$ need to ensure that

$$H(s) = \frac{G_{p1}(s)M(s)}{C(s)G_{p1}(s) + (1 - C(s))M(s)} \tag{25}$$

is stable and

$$\|G(s)\|_{\mathcal{L}_1} L < 1\,, \tag{26}$$

where

$$G(s) = H(s)(1 - C(s))\,, \tag{27}$$

and L is the Lipschitz constant of $z_1(t)$ w.r.t. $u_\theta(t)$.

Here, we note that we need to find suitable m and ω to stabilize $H(s)$ in (25). The condition in (26) is always satisfied for the system G_{p1}, since $z_1(t)$ does not depend on $u_\theta(t)$, which renders $L = 0$. In general, this may not be true.

C. Closed-loop Reference System

Consider the following closed-loop reference system:

$$u_{\theta_{ref}}(s) = M(s)(u_{1_{ref}}(s) + \sigma_{ref}(s)), \quad (28)$$

$$\sigma_{ref}(s) = \frac{(G_{p1}(s) - M(s))u_{1_{ref}}(s) + G_{p1}(s)z_1(s)}{M(s)}, \quad (29)$$

$$u_{1_{ref}}(s) = u_{\theta_c}(s) - C(s)\sigma_{ref}(s)\,. \quad (30)$$

It follows from [1] that for any given $M(s)$ and $C(s)$, there exist constants $\gamma_1 > 0, \gamma_2 > 0$ leading to the following result.

Lemma 2: Given the system in (15) and the $\mathcal{L}_1$ adaptive controller defined via (21), (22) and (23) subject to (26), we have:

$$\|u_\theta - u_{\theta_{ref}}\|_{\mathcal{L}_\infty} \leq \frac{\gamma_1}{\sqrt{\Gamma_c}}\,, \quad (31)$$

$$\|u_1 - u_{1_{ref}}\|_{\mathcal{L}_\infty} \leq \frac{\gamma_2}{\sqrt{\Gamma_c}}\,. \quad (32)$$

It follows from Lemma 2 that by increasing the adaptation rate Γ_c, we can render the bounds between the input/output signals of the closed-loop adaptive system and the reference system arbitrarily small.

D. Desired Low-pass system

We now derive the bounds between the signals of the closed-loop reference system and the desired system in (18). Let

$$y_{des}(s) = \begin{bmatrix} u_{\theta_{des}}(s) \\ u_{\psi_{des}}(s) \end{bmatrix} = M(s)y_c(s)\,. \quad (33)$$

Lemma 3: Given the systems in (28)-(30) and (33), we have:

$$\|u_{\theta_{des}} - u_{\theta_{ref}}\|_{\mathcal{L}_\infty} \leq \gamma_3\,, \quad (34)$$

where

$$\gamma_3 = \|H(s) - M(s)\|_{\mathcal{L}_1}\|u_{\theta_c}\|_{\mathcal{L}_\infty} + \|G(s)\|_{\mathcal{L}_1}L_{10}. \quad (35)$$

Proof. It follows from (29)-(30) that

$$u_{1_{ref}}(s) = u_{\theta_c}(s) - C(s)\frac{(G_{p1}(s) - M(s))u_{1_{ref}}(s) + G_{p1}(s)z_1(s)}{M(s)}\,,$$

and hence

$$u_{1_{ref}}(s) = \frac{M(s)u_{\theta_c}(s) - C(s)G_{p1}(s)z_1(s)}{C(s)G_{p1}(s) + (1 - C(s))M(s)}\,. \quad (36)$$

It follows from (28)-(29) that

$$u_{\theta_{ref}}(s) = G_{p1}(s)(u_{1_{ref}}(s) + z_1(s))\,. \quad (37)$$

Substituting (36) into (37), it follows from (25) that

$$\begin{aligned} u_{\theta_{ref}}(s) &= G_{p1}(s)\Big(\frac{M(s)u_{\theta_c}(s) - C(s)G_{p1}(s)z_1(s)}{C(s)G_{p1}(s) + (1 - C(s))M(s)} \\ &\quad + z_F(s)\Big) \\ &= G_{p1}(s)M(s)\left(\frac{u_{\theta_c}(s) + (1 - C(s))z_1(s)}{C(s)G_{p1}(s) + (1 - C(s))M(s)}\right) \\ &= H(s)\left(u_{\theta_c}(s) + (1 - C(s))z_F(s)\right)\,. \end{aligned} \quad (38)$$

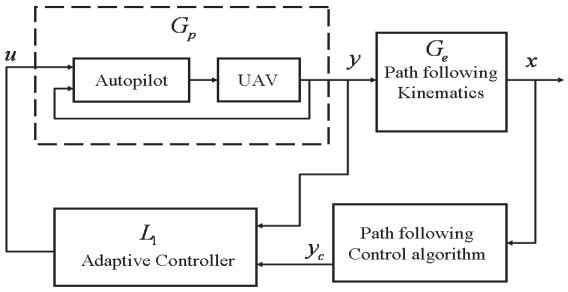

Fig. 3. $\mathcal{L}_1$ adaptive controller for the cascaded systems

It follows from (33) and (38) that

$$\begin{aligned} u_{\theta_{ref}}(s) - u_{\theta_{des}}(s) &= (H(s) - M(s))u_{\theta_c}(s) \\ &\quad + H(s)(1 - C(s))z_1(s)\,. \end{aligned}$$

Since $H(s)$ is strictly proper and stable, it follows from (27) that $G(s)$ is also strictly proper and stable and hence

$$\begin{aligned} \|u_{\theta_{ref}} - u_{\theta_{des}}\|_{\mathcal{L}_\infty} \leq \|H(s) - M(s)\|_{\mathcal{L}_1}\|u_{\theta_c}\|_{\mathcal{L}_\infty} + \\ \|H(s)(1 - C(s))\|_{\mathcal{L}_1}\|z_1\|_{\mathcal{L}_\infty}\,. \end{aligned} \quad (39)$$

Therefore, the relationship in (34) follows from (35) and (39), which proves the Lemma. □

Let

$$\tilde{y}(t) \triangleq [\tilde{u}_\theta(t) \;\; \tilde{u}_\psi(t)]^\top = y(t) - y_{des}(t)\,. \quad (40)$$

Lemma 4: Given the $\mathcal{L}_1$ adaptive controller defined via (21), (22) and (23) subject to (26), we have:

$$\|\tilde{u}_\theta\|_{\mathcal{L}_\infty} \leq \bar{\gamma}_1\,, \quad (41)$$

where $\bar{\gamma}_1 = \gamma_1/\sqrt{\Gamma_c} + \gamma_3$.

The proof of Lemma 4 follows from Lemmas 2 and 3 directly. Similarly, if we implement $\mathcal{L}_1$ adaptive controller for the system in (15), we have

$$\|\tilde{u}_\psi\|_{\mathcal{L}_\infty} \leq \bar{\gamma}_2\,, \quad (42)$$

where $\bar{\gamma}_2 > 0$ is a constant similar to $\bar{\gamma}_1$.

It we further want to reduce the bounds of $\bar{\gamma}_1$ and $\bar{\gamma}_2$, we need to choose ω and Γ_c large. It follows that

$$\lim_{\Gamma_c \to \infty}\left(\gamma_1/\sqrt{\Gamma_c} + \lim_{\omega \to \infty}\gamma_3\right) = 0\,,$$

and hence $\lim_{\omega \to \infty, \Gamma_c \to \infty} \bar{\gamma}_i = 0, \;\; i = 1, 2\,.$

E. Control of cascaded systems

The cascaded closed-loop system defined via (8) (21), (22) and (23) is illustrated in Figure 3. Stabilization of the cascaded system is proved next.

Theorem 1: Given the cascaded controller defined via (8) (21), (22) and (23), the closed-loop system in (6) and (15)-(15) can be stabilized by appropriate choice of m, ω, Γ_c.

Proof. Let

$$V = V_c(x(t)) + (y(t) - y_c(t))^\top (y(t) - y_c(t))/2 \quad (43)$$

be the candidate Lyapunov function. Then

$$\begin{aligned}\dot{V}(t) = {} & \frac{x_F}{c_1}(-\dot{\tau}(1-\kappa(\tau)y_F) + v\cos(\theta_e)\cos(\psi_e)) \\ & + \frac{y_F}{c_1}(-\dot{\tau}(\kappa(\tau)x_F - \zeta(\tau)z_F) + v\cos(\theta_e)\sin(\psi_e)) \\ & + \frac{z_F}{c_1}(-\zeta(\tau)\dot{\tau}y_F - v\sin(\theta_e)) + \frac{\theta_e - \delta_\theta}{c_2}(u_{\theta_c} - \dot{\delta}_\theta) \\ & + \frac{\psi_e - \delta_\psi}{c_3}(u_{\psi_c} - \dot{\delta}_\psi) + \frac{\theta_e - \delta_\theta}{c_2}(u_\theta - u_{\theta_c}) + \\ & \frac{\psi_e - \delta_\psi}{c_3}(u_\psi - u_{\psi_c}) + (y - y_c)^\top(\dot{y} - \dot{y}_c)\,. \end{aligned} \quad (44)$$

Using the same steps of Lemma 1, it follows that

$$\begin{aligned}\dot{V}(t) \le {} & -x^\top Q_c x + \frac{\theta_e - \delta_\theta}{c_2}(u_\theta - u_{\theta_c}) + \\ & \frac{\psi_e - \delta_\psi}{c_3}(u_\psi - u_{\psi_c}) + (y - y_c)^\top(\dot{y} - \dot{y}_c)\,, \end{aligned} \quad (45)$$

where Q_c is defined in (13). Letting

$$\begin{aligned} x_1(t) &= [x_F(t) \;\; y_F(t) \;\; z_F(t)]^\top, \\ x_2(t) &= [\theta_e(t) - \delta_\theta(t) \;\; \psi_e(t) - \delta_\psi(t)]^\top, \\ Q_{c1} &= \mathrm{diag}\Big(\frac{K_1}{c_1} \;\; \frac{v_{\min}}{c_1(|y_{F_{\max}}| + d_2)} \\ &\qquad \frac{v_{\min}}{c_1(|z_{F_{\max}}| + d_1)}\Big), \\ Q_{c2} &= \mathrm{diag}\Big(\frac{K_2}{c_2} \;\; \frac{K_3}{c_3}\Big), \\ Q_{c3} &= \mathrm{diag}\Big(\frac{1}{c_2} \;\; \frac{1}{c_3}\Big), \end{aligned} \quad (46)$$

it follows from (45) that

$$\begin{aligned}\dot{V}(t) \le {} & -x_1^\top Q_{c1}x_1 - x_2^\top Q_{c2}x_2 + x_2^\top Q_{c3}(y - y_c) + \\ & (y - y_c)^\top(\dot{y} - \dot{y}_c)\,. \end{aligned} \quad (47)$$

From (33), we have that

$$\dot{y}_{des}(t) = -m y_{des}(t) + m y_c(t). \quad (48)$$

From (40) and (48), it can be computed that

$$\begin{aligned}(y - y_c)^\top(\dot{y} - \dot{y}_c) &= (y - y_c)^\top(\dot{\tilde{y}} - \dot{y}_c) + (y - y_c)^\top(\dot{y}_{des}) \\ &= (y - y_c)^\top(\dot{\tilde{y}} - \dot{y}_c) + (y - y_c)^\top(-m y_{des} + m y_c) \\ = (y - y_c)^\top(\dot{\tilde{y}} - \dot{y}_c) &- m(y - y_c)^\top(y - y_c) + m(y - y_c)^\top\tilde{y}\,. \end{aligned}$$

It follows from (47) that

$$\begin{aligned}\dot{V}(t) \le {} & -x_1^\top Q_{c1}x_1 - x_2^\top Q_{c2}x_2 + x_2^\top Q_{c3}(y - y_c) - \\ & m(y - y_c)^\top(y - y_c) + (y - y_c)^\top(\dot{\tilde{y}} - \dot{y}_c + m\tilde{y})\,. \end{aligned}$$

Let $r(t) = \dot{\tilde{y}}(t) - \dot{y}_c(t) + m\tilde{y}(t)$. We note that both $y(t)$ and $y_{des}(t)$ are low-pass filtered signals, and hence $\tilde{y}(t)$ is bounded. Similarly, the control law in (8) implies that $y_c(t)$ has a bounded derivative. Lemma 4 implies that $m\tilde{y}(t)$ is bounded for any m, and therefore $r(t)$ is bounded, i.e. $\exists\ \gamma_4$, such that

$$r^\top(t)r(t) \le \gamma_4\,, \quad \gamma_4 > 0. \quad (49)$$

Letting $\chi = [x_1^\top \;\; x_2^\top \;\; (y - y_c)^\top \;\; r^\top]^\top$, one can compute

$$\dot{V}(t) \le -\chi^\top(t)\bar{Q}\chi(t) + \gamma_5 r^\top(t)r(t)\,, \quad (50)$$

where

$$\bar{Q} = \begin{bmatrix} Q_{c1} & 0 & 0 & 0 \\ 0 & Q_{c2} & -Q_{c3}/2 & 0 \\ 0 & -Q_{c3}/2 & m\mathbb{I} & -\mathbb{I}/2 \\ 0 & 0 & -\mathbb{I}/2 & \gamma_5\mathbb{I} \end{bmatrix} \quad (51)$$

with $\mathbb{I}$ being the identity matrix of appropriate dimension. For any $\gamma_5 > 0$, the choice of m

$$m\mathbb{I} > \frac{Q_{c3}^2}{4Q_{c2}} + \frac{1}{4\gamma_5}\mathbb{I} \quad (52)$$

will lead to $\bar{Q} > 0$ and hence (49) and (50) imply that $\dot{V}(t) \le -\chi^\top(t)\bar{Q}\chi(t) + \gamma_4\gamma_5$. Thus, as long as $\chi^\top(t)\bar{Q}\chi(t) > \gamma_4\gamma_5$, we have $\dot{V}(t) < 0$. It implies that $V(t)$ will keep decreasing until $\chi^\top(t)\bar{Q}\chi(t) \le \gamma_4\gamma_5$, and hence the closed-loop cascaded system is ultimately bounded. □

Note that for any γ_5, (52) can always be satisfied by increasing m, which implies that the ultimate bound of x can be rendered small with large m. Further, it follows from Lemma 4 that the bound for γ_4 can be reduced by increasing ω and Γ_c. However, ω cannot be chosen arbitrarily large due to the limited bandwidth of the control channel of $\mathcal{G}_p$. For more details on the possible choices of ω and m see [9].

V. Flight Test Results

The complete path following control system, shown in Fig. 3, was implemented on an experimental UAV Rascal operated by NPS. The cascaded controller defined in (8) (21), (22) and (23) with

$$M(s) = \frac{1}{10s+1}, \quad C(s) = \frac{1}{10s+1}, \quad \Gamma = 10$$

was flight tested in February 2007. The subsystem $\mathcal{G}_p$ represents Rascal with the Piccolo autopilot as described in [2]. Fig. 4 presents the implementation architecture.

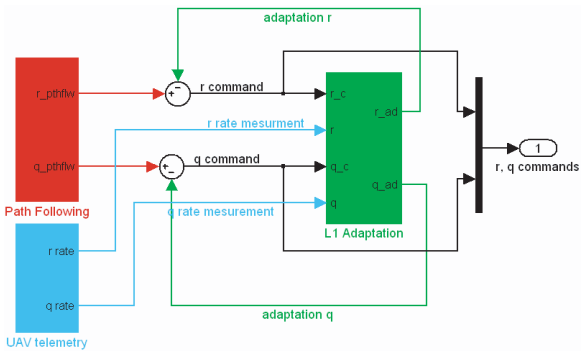

Fig. 4. Flight Test System Architecture

Fig. 5 presents the phase portrait, i.e. the position $(x_I(t), y_I(t))$ in the inertial frame I as introduced in (3). The UAV flight trajectory is compared to the desired trajectory. Fig. 6 shows the corresponding time trajectories along with the commanded rate input for the autopilot. It can be seen

that the maximum deviation from the desired trajectory is about $40m$, which corresponds to the point of the sharp turn. Other than at this point, the tracking errors are very close to zero. Flight test results without $\mathcal{L}_1$ adaptive controller are plotted in Figs. 7 and 8 for comparison.

VI. Conclusion

A complete inner-outer loop path following architecture is presented that relies on $\mathcal{L}_1$ adaptive output feedback to augment an existing autopilot. This architecture enables a UAV with an off-the-shelf autopilot to follow a predetermined path that it was not otherwise designed to follow. The paper provides analytically computable performance bounds.

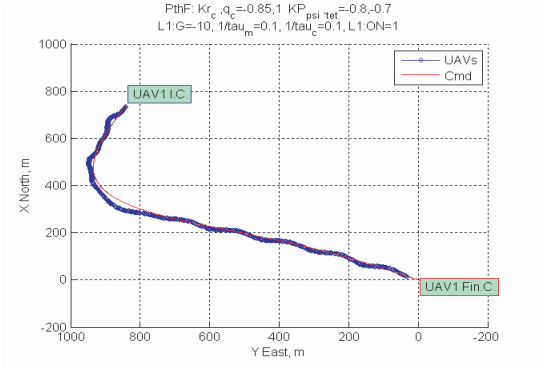

Fig. 5. Desired and actual UAV trajectories from flight test with $\mathcal{L}_1$ adaptive controller

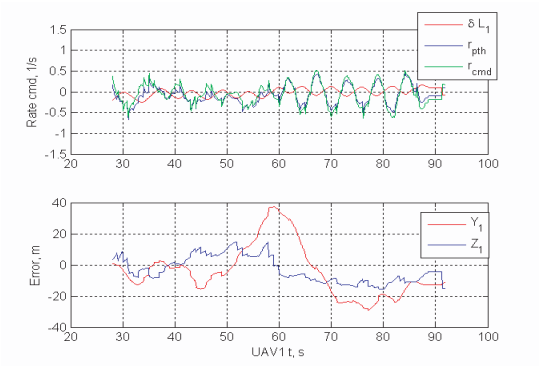

Fig. 6. Top: path following turn rate command and contributions from outer loop and $\mathcal{L}_1$ adaptation; bottom: path following errors

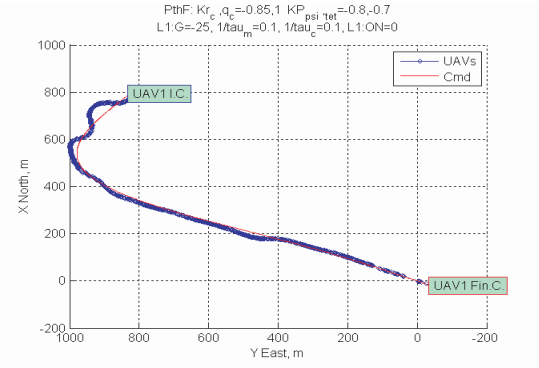

Fig. 7. Actual and desired UAV trajectories without adaptation

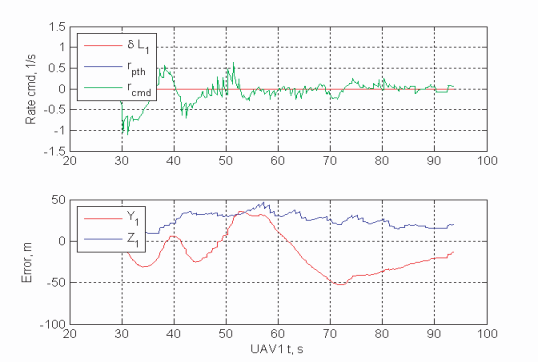

Fig. 8. Top: path following turn rate command without adaptation; bottom: path following errors

References

[1] C. Cao and N. Hovakimyan. $\mathcal{L}_1$ adaptive output feedback controller for systems of unknown dimension. *American Control Conference*, 2007.

[2] I. Kaminer, O. Yakimenko, A. Pascoal, and R. Ghabcheloo. Path generation, path following and coordinated control for timecritical missions of multiple UAVs. *American Control Conference*, pages 4906 – 4913, June 2006.

[3] C. Cao and N. Hovakimyan. Design and analysis of a novel $\mathcal{L}_1$ adatpive control architecture, Part I: Control signal and symptotic stability. *In Proc. of American Control Conference*, pages 3397–3402, 2006.

[4] C. Cao and N. Hovakimyan. Design and analysis of a novel $\mathcal{L}_1$ adatpive control architecture, Part II: Guaranteed transient performance. *In Proc. of American Control Conference*, pages 3403–3408, 2006.

[5] C. Cao and N. Hovakimyan. $\mathcal{L}_1$ adaptive output feedback controller for systems with time-varying unknown parameters and bounded disturbances. *American Control Conference*, 2007.

[6] C. Cao and N. Hovakimyan. Guaranteed transient performance with $\mathcal{L}_1$ adaptive controller for systems with unknown time-varying parameters: Part I. *American Control Conference*, 2007.

[7] C. Cao and N. Hovakimyan. Stability margins of $\mathcal{L}_1$ adaptive controller: Part II. *American Control Conference*, 2007.

[8] I. Kaminer, O. Yakimenko, V. Dobrokhodov, A. Pascoal, N. Hovakimyan, V. V. Patel, C. Cao, and A. Young. Coordinated path following for time-critical missions of multiple UAVs via $\mathcal{L}_1$ adaptive output feedback controllers. *AIAA Guidance, Navigation and Control Conference, Hilton Head Island, SC*, August 2007.

[9] R. Hindman, C. Cao, and N. Hovakimyan. Design of high-performance, stable $\mathcal{L}_1$ adaptive output feedback controller. In *Proc. of AIAA Guidance, Navigation & Control Conf.*, Hilton Head Island, SC, 2007.